Macromolecules 1985, *18*, 1741–1745

Light Scattering Study of Three-Component Systems. 2. Thermodynamic Analyses of Poly(methyl methacrylate) in the Binary Mixture 1-Chlorobutane + 2-Methoxyethanol

Mitsuo Nakata* and Naoko Numasawa[†]

Department of Polymer Science, Faculty of Science, Hokkaido University, Sapporo, Japan.
Received November 26, 1984

ABSTRACT: The second virial coefficients for poly(methyl methacrylate) ($M_w = 2.44 \times 10^6$) in the mixed solvent 1-chlorobutane (BuCl) + 2-methoxyethanol (MOEt) were compared with the generalized Flory–Huggins equation. The binary interaction function for the mixed solvent was determined as a function of the volume fraction u_2 of MOEt in the mixed solvent by using the experimental data of the heat of mixing and the boiling temperature. The second virial coefficients were calculated from the observed binary interaction functions with a rigorous thermodynamic relation for the three-component system. The calculated second virial coefficients were about 8 times larger than the observed ones except in the region $u_2 < 0.2$, where the calculated values were negative, opposite to the observed ones. An agreement between the observed and the calculated second virial coefficients was obtained by introducing a ternary function $g_T(u_2,\phi_3)$ as a function of u_2 and the volume fraction ϕ_3 of polymer. A reasonable agreement was not obtained by the function $g_T(u_2)$ independent of ϕ_3, especially at small u_2.

I. Introduction

The thermodynamic properties of ternary systems of a polymer in a mixed solvent are usually very different from those of binary systems of the polymer in the component solvents.[1–6] The solvent power of nonsolvents is found to increase upon addition of a small amount of nonsolvent or poor solvent.[3,6] Some mixtures of two nonsolvents for a polymer act as a moderately good solvent for the polymer. The synergistic behavior, called cosolvency,[2,3] is characteristic of systems of polymer + mixed solvent. Thermodynamic treatments for polymers in mixed solvents have been developed for three-component systems.[7–12] The expansion factors for a polymer coil calculated with a Shulz–Flory relation[9] as well as with the single-liquid approximation of Scott[8] were found to be much larger, for instance about 10 times, than the experimental values obtained by viscosity measurements.[13,14] Wolf et al. made phase equilibrium measurements on the cosolvent systems of poly(methyl methacrylate) (PMMA) + mixed solvent[3] and polystyrene (PS) + mixed solvent[4] and explained the experimental results with a combination of the Prigogine–Patterson theory[15–17] and the single-liquid approximation of Scott. Horta et al. made light scattering measurements[18] and phase equilibrium measurements[6] on the cosolvent system PMMA + acetonitrile + 1-chlorobutane. By use of the single-liquid approximation, the observed second virial coefficients and the critical lines were compared with the Flory–Patterson–Prigogine theory[19] and with the solubility parameter theory, respectively.

According to the single-liquid approximation, ternary systems of polymer + mixed solvent can be treated in an analogous way as binary systems with a single interaction parameter. In this simplified treatment, however, we could understand the characteristic behavior of ternary systems of polymer + mixed solvent only in a qualitative way, because the errors due to the single-liquid approximation are obscure, especially in cosolvent systems. Šolc et al. derived equations for the preferential adsorption coefficient and the second virial coefficient using the Gibbs free energy of the three-component system.[12] They analyzed experimental data of dialysis equilibrium and intrinsic viscosity on the system PMMA + benzene + methanol and introduced a composition-dependent ternary parameter to obtain an agreement between the theories and the experimental data. A ternary parameter was also required to explain light scattering data for the preferential adsorption measured on the system PS + benzene + cyclohexane.[10] Munk et al.[20,21] derived equations for the preferential adsorption coefficient and the second virial coefficient with a refined treatment for the three-component systems and made comparisons with experimental data on systems of polystyrene + mixed solvent. They made detailed thermodynamic analyses of the solvent mixtures to obtain the binary interaction functions and evaluated the ternary functions from the data of the preferential adsorption coefficient and the second virial coefficient. Recently, Horta et al. made light scattering measurements on PMMA in cosolvents.[22] The observed second virial coefficients were explained by the Flory–Patterson–Prigogine theory combined with the single-liquid approximation. However, the theory failed to give a consistent explanation of the observed preferential adsorption coefficients.

In the previous paper,[23] we made light scattering measurements on the ternary system PMMA + 2-methoxyethanol (MOEt) + 1-chlorobutane (BuCl). The observed second virial coefficients and the mean-square radii of gyration did not show a behavior characteristic of the mixed solvent in the framework of the two-parameter theory. The mixed solvent was found to be a good solvent from the large excluded volume of PMMA, though BuCl is a poor solvent and MOEt is a moderate solvent for PMMA. Because of this synergistic behavior the mixture BuCl + MOEt could be taken as a cosolvent pair for PMMA. In this study, we have compared the corrected second virial coefficients in the mixed solvent with the generalized Flory–Higgins equation by using the thermodynamic relation of the three-component system derived by Munk et al.[20] The Gibbs free energy for the mixture BuCl + MOEt was determined by measuring heats of mixing and boiling temperatures.

II. Experimental Section

A. Heats of Mixing of the Mixture BuCl + MOEt. The heat of mixing of the mixture BuCl + MOEt was determined by measuring the temperature change on mixing. A polyethylene bottle with thin wall and breakable bottom was filled with a solvent sample of larger volume. The bottle was set in thermal contact with another solvent sample in a Dewar vessel, which was equipped with a Beckmann thermometer, a stirring fan, and a thick lid of foam polystyrene. The total volume of BuCl and MOEt was 100 mL. The Dewar vessel was set in an air bath

---

[†] Present address: Department of Polymer Chemistry, Tokyo Institute of Technology, Ookayama, Meguro-ku, Tokyo 152, Japan.

0024-9297/85/2218-1741$01.50/0

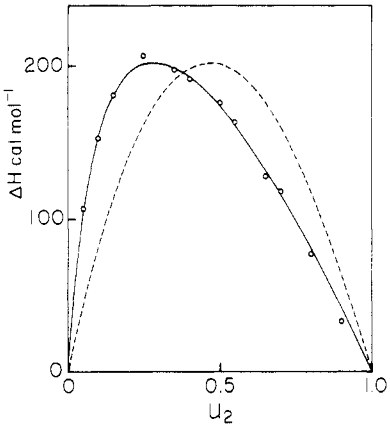

Figure 1. Heats of mixing per mole (ΔH (cal/mol)) as a function of the volume fraction u_2 for the binary mixture 1-chlorobutane (1) + 2-methoxyethanol (2) at 40 °C. Solid curve is calculated from eq 17 and 18 and broken curve from eq 17 with $h_{12} = 473$.

thermostated within ±0.02 K at 40 °C. After attainment of thermal equilibrium the bottom of the bottle was broken by a thin glass rod and the temperature change on mixing was measured by the Beckmann thermometer. A maximum decrease of temperature was read about 40 s after the onset of mixing and a slow increase of temperature followed due to heat flow from the Dewar vessel. From the maximum change of temperature, which was usually a few degrees, we calculated the heat of mixing by using the molar heat capacity of the mixture estimated with the assumption of additivity of those of each component. The molar heat capacities of each component were evaluated according to the group-contribution method of Missenard.[24] Since the heat of mixing thus obtained was considerably affected by the heat flow from the Dewar vessel and by a rather slow response of the Beckmann thermometer to temperature change, we made measurements on binary mixtures of known heats of mixing to correct the data. The plot of the known heat of mixing vs. the product of the maximum change of temperature and the heat capacity was represented by a straight line and the slope was used for the correction. The accuracy of the corrected heat of mixing for the mixture BuCl + MOEt was inferred to be ±5%, though the precision of the experimental data was much better than this accuracy. Figure 1 gives the heats of mixing per mole as a function of the volume fraction u_2 of MOEt. The open circles represent the experimental data.

B. Boiling Temperatures of the Mixture BuCl + MOEt. Boiling temperatures of the mixture BuCl + MOEt were measured as a function of the composition at the reduced pressure 200.0 ± 0.3 mmHg. The glass apparatus for the measurements consists of a flask of 100 mL with a neck of 50 cm in length, a condenser, and a container for small pieces of broken china. The container was attached at the top of the apparatus to supply dried pieces of china to the mixture in the flask without opening the system. A mercury thermometer was placed inside the flask and its location was changed by magnets. The flask filled with sample liquid of 50 mL was heated by a mantle heater. For pure liquids, BuCl and MOEt, the boiling temperature in the vapor phase was uniform in the flask and was not affected by heating rate. This temperature was found to agree with literature values. For the mixtures the temperature in the vapor phase decreased with the distance from the liquid–vapor interface. Hence, we determined the boiling temperature for the mixtures as the temperature at which the mixtures ceased boiling on lowering temperature. In observing the lower limit of boiling temperature, boiling was stimulated by supplying fresh pieces of china and tapping the flask to minimize superheating. For pure liquids the lower limit of the boiling temperature was higher by 0.2 °C than the temperature in the vapor phase. In Figure 2a the observed boiling temperatures are plotted against the volume fraction u_2 of MOEt.

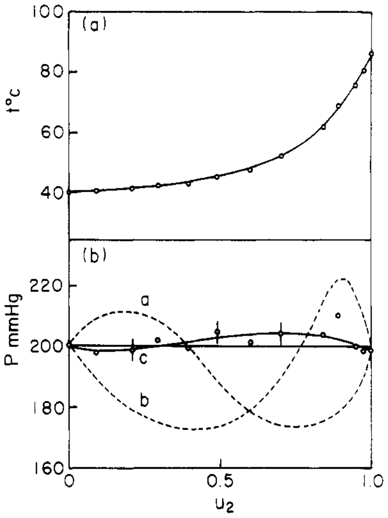

Figure 2. (a) Plot of boiling temperature observed at 200 mmHg against the volume fraction u_2 for the binary mixture 1-chlorobutane (1) + 2-methoxyethanol (2). (b) Total vapor pressure calculated from the boiling temperature. Broken curve a is due to $g_{12} = h_{12}/T$. Broken curve b is due to $g_{12} = 1.51(T_0/T)$. Solid curve c is due to eq 22. Vertical bars for the calculated points correspond to the boiling temperature variation of ±0.5 °C.

III. Phenomenological Equations of Three-Component Systems

In thermodynamic equations of multicomponent systems various compositions are employed such as the volume fraction ϕ_i, the number of moles N_i, the concentration c_i, and the molality m_i. According to fluctuation theories, light scattering at zero angle arising from composition fluctuations of polymer molecules in the three-component system solvent (1) + solvent (2) + polymer (3) can be written as[10,25-27]

$$R_0 = K'(\partial n/\partial c_3)_{u_2}{}^2[RTc_3/(\partial \Pi/\partial c_3)_\mu] \times [1 - \lambda(\partial n/\partial u_2)_0/(\partial n/\partial c_3)_{u_2}]^2 \quad (1)$$

where

$$K' = 2\pi^2 n^2/(N_A \lambda_0{}^4)$$

where n is the refractive index of the system, N_A is Avogadro's number, λ_0 is the wavelength in a vacuum, RT has its usual meaning, and u_2 is the volume fraction of component 2 in the mixed solvent ($u_2 = \phi_2/(\phi_1 + \phi_2)$). The derivative $(\partial n/\partial u_2)_0$ is taken at the limit $c_3 = 0$. The osmotic pressure Π and the preferential adsorption coefficient λ in eq 1 can be represented with the derivatives $a_{ij} = (\partial \mu_i/\partial m_j)_{T,P,m_{k\neq j}}$ of the chemical potential μ_i, where the molality m_i is defined by moles per unit mass of component 1. The equations for Π and λ are written as

$$(\partial \Pi/\partial c_3)_\mu = (V_m c_3)(M_1 M_3{}^2 N_1)(a_{22}a_{33} - a_{23}{}^2)/a_{22} \quad (2)$$

$$\lambda = (1 - \phi_2)(\bar{V}_2/\bar{V}_3)\bar{v}_3(a_{23}/a_{22}) \quad (3)$$

Here, M_i and $\bar{V}_i$ are the molecular weight and the partial molar volume of component i, respectively, $\bar{v}_3$ is the partial specific volume of the polymer, and V_m is the total volume of the system. At low polymer concentration the osmotic pressure can be expanded in powers of the concentration c_3 as

$$(\partial \Pi/\partial c_3)_\mu = RT(1/M_3 + 2A_2 c_3 + ...) \quad (4)$$

where A_2 is the second virial coefficient. Equations 1 and 4 show that the measurements of R_0, $(\partial n/\partial c_3)_{u_2}$, and $(\partial n/\partial u_2)_0$ give A_2 and λ, provided M_3 is known. In the case of $(\partial n/\partial u_2)_0 = 0$, eq 1 reduces to the equation for binary systems of polymer + single solvent and the experimental data can be analyzed as in the case of two-component systems.

The preferential adsorption coefficient λ and the second virial coefficient A_2 can be derived from the analytical expression for the Gibbs free energy of mixing ΔG_{mix}. For an equation of ΔG_{mix} Pouchlý et al.[12] and Munk et al.[20] have employed a generalized expression of the Flory–Huggins equation[28] given by

$$\Delta G_{\mathrm{mix}}/NRT = \phi_1 \ln \phi_1 + (\phi_2/r_2) \ln \phi_2 + (\phi_3/r_3) \ln \phi_3 + g_{12}(u_2)\phi_1\phi_2 + g_{13}(\phi_3)\phi_1\phi_3 + g_{23}(\phi_3)(\phi_2/r_2)\phi_3 + g_{\mathrm{T}}(u_2,\phi_3)\phi_1\phi_2\phi_3 \quad (5)$$

where r_2 and r_3 are the ratios of partial molar volumes of solvent component 2 and polymer component 3 to that of solvent component 1, and N $(=N_1 + r_2N_2 + r_3N_3)$ is the total number of moles of lattice sites. The binary interaction function g_{ij} in eq 5 covers all the thermodynamic properties of the binary system of components i and j. The function g_{T} covers all deviations of the real system from the idealized system which can be represented by the binary interaction functions g_{ij}. As the function g_{T} in eq 5 is multiplied by a product of three volume fractions, we refer to the function as a ternary function. We use eq 5 as a phenomenological equation in the sense that the binary interaction functions are to be evaluated from experimental data and that the ternary function g_{T} should be considered to be defined by eq 5. By substituting eq 5 into eq 2 and 3 Munk et al. derived the explicit expressions for A_2 and λ in the form

$$A_2^0 = [\bar{v}_3^2/(2\bar{V}_1)][(b_{22}b_{33} - b_{23}^2\phi_1\phi_2)/b_{22}] \quad (6)$$

$$\lambda^0 = \bar{v}_3(b_{23}/b_{22})\phi_1\phi_2 \quad (7)$$

where the superscript zero on A_2 and λ refers to the lattice theory as a base of eq 5, and the b_{ij} are given by

$$b_{22} = (1/r_2)\phi_1 + \phi_2 - \phi_1\phi_2[2g_{12} - 2(\phi_1 - \phi_2)(\partial g_{12}/\partial u_2) - \phi_1\phi_2(\partial^2 g_{12}/\partial u_2^2)] \quad (8)$$

$$b_{23} = 1 - (1/r_2) + (1/r_2)g_{23}° - g_{13}° - (\phi_1 - \phi_2)(g_{12} - g_{\mathrm{T}}°) + \phi_1\phi_2[(\partial g_{\mathrm{T}}/\partial u_2)° - (\partial g_{12}/\partial u_2)] \quad (9)$$

$$b_{33} = \phi_1 + (1/r_2)\phi_2 + 2\phi_1\phi_2[(g_{12} - g_{\mathrm{T}}°) - \chi_{\mathrm{T}}°] - 2[(1/r_2)\chi_{23}°\phi_2 + \chi_{13}°\phi_1] \quad (10)$$

with

$$\chi_{i3}° = g_{i3}° - (\partial g_{i3}/\partial \phi_3)° \quad (11)$$

$$\chi_{\mathrm{T}}° = g_{\mathrm{T}}° - (\partial g_{\mathrm{T}}/\partial \phi_3)° \quad (12)$$

Here, the superscript zero on the right-hand side of eq 9–12 refers to the limit of zero polymer concentration. The terms inversely proportional to r_3 are neglected in eq 9 and 10. Equations 8–10 are the same as those obtained by Munk et al.[20] when r_2 is replaced by the inverse of l in their equations. It is noticed that eq 2 for the osmotic pressure is slightly different from that derived by Munk et al. However, the magnitude of this difference is of the order of the inverse of r_3 at low polymer concentration and, therefore, the second virial coefficients calculated from these two equations agree with each other. For the binary system polymer + single solvent i, eq 6 reduces to

$$A_{2,i}° = (\bar{v}_3^2/\bar{V}_i)(1/2 - \chi_{i3}°) \quad (13)$$

Within the scope of the lattice theory, the functional form of g_{i3} may be written as

$$g_{i3} = g_{i3}°/[1 - (2/z)\phi_3] \quad (14)$$

where z is the coordination number of the lattice. Equation 14 is convenient to determine g_{i3} from the experimental data of $A_{2,i}$, because eq 11 and 14 yield the relation

$$\chi_{i3}° = (1 - 2/z)g_{i3}° \quad (15)$$

We employed $z = 8$ in the data analyses. The binary interaction function g_{12} could be estimated from thermodynamic data such as the vapor pressure and the heats of mixing.

The second virial coefficient A_2 in single solvents can be written in the form[29]

$$A_2 = A_2°h(z/\alpha^3) \quad (16)$$

where the function $h(z/\alpha^3)$ represents the effect of the excluded volume and $A_2°$ is defined in the previous paper.[23] We showed that the excluded volume effect in the ternary system BuCl (1) + MOEt (2) + PMMA (3) is not different from those of systems of polymer + single solvent in the framework of the two-parameter theory and that the characteristic feature of the system is represented by $A_2°$ in eq 16 as a function of u_2.[23] This indicates that the expression of eq 16 is pertinent to the present ternary system and $A_2°$ in eq 16 can be compared with eq 6. We have evaluated the values of $A_2°$ for the present system with the Kurata–Yamakawa theory for the function h as given in Table I in the previous paper.

IV. Evaluation of the Binary Interaction Functions

For the comparison of eq 6 and the experimental values we must begin with a determination of the binary interaction function g_{ij}. From the values of $A_2° = 0$ at $u_2 = 0$ and $A_2° = 1.64 \times 10^{-4}$ at $u_2 = 1$ we obtain $g_{13}° = 0.667$ and $g_{23}° = 0.642$, respectively, by using eq 13 and 15 for $z = 8$. Here, we employed $\bar{v}_3 = 0.838$ mL/g, $\bar{V}_1 = 107.1$ mL/mol, and $\bar{V}_2 = 80.4$ mL/mol, which were estimated with the values for pure substances. These values yield molar volume ratios $r_2 = 0.751$ and $r_3 = 1.91 \times 10^4$.

Next, we must analyze the data of the heats of mixing and the boiling temperature for the system BuCl + MOEt to evaluate the function g_{12}. Heats of mixing can be expressed as

$$\Delta H = Rh_{12}N_1u_2 \quad (17)$$

The observed heats of mixing for the system BuCl + MOEt were found to be well represented by the empirical relation

$$h_{12} = 146 + 162/(0.119 + u_2) \quad (18)$$

which describes the asymmetric behavior of ΔH. The solid curve in Figure 1 is described by eq 18. The broken curve of symmetry was illustrated by the constant $h_{12} = 473$.

The total vapor pressure p of binary mixtures is given by the equation

$$p = p_1 \exp(\Delta\mu_1/RT) + p_2 \exp(\Delta\mu_2/RT) \quad (19)$$

where p_1 and p_2 are the vapor pressures for the pure components. The excess chemical potentials $\Delta\mu_1$ and $\Delta\mu_2$ in eq 19 are derived from the Gibbs free energy of mixing

$$\Delta G_{\mathrm{mix}}/RT = N_1 \ln (1 - u_2) + N_2 \ln u_2 + g_{12}(T,u_2)N_1u_2 \quad (20)$$

The function $g_{12}(T,u_2)$ of the system BuCl + MOEt is obtained from the Gibbs–Helmholtz equation $((\partial g_{12}/\partial T)_{p,u_2} = -h_{12}/T^2)$ as

$$g_{12}(T,u_2) = (T_0/T - 1)h_{12}/T_0 + g_{12}(T_0,u_2) \quad (21)$$

where $T_0 = 313.2$ K and the function h_{12}, which is assumed to be independent of temperature, is given by eq 18. Since the vapor pressures as a function of temperature for BuCl and MOEt are given in the literature, the total vapor pressure p can be calculated from the observed boiling temperature, provided that the function $g_{12}(T,u_2)$ is known.

First, we calculated the total vapor pressure by assuming $g_{12} = h_{12}/T$, which results from neglect of the entropy term in eq 21. The calculations are given by broken curve a in Figure 2b. The calculated vapor pressures are found to

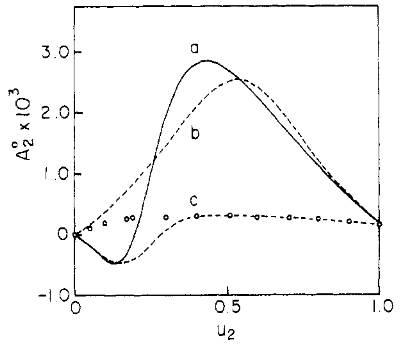

Figure 3. Plot of A_2° against the volume fraction u_2 of 2-methoxyethanol. Open circles represent the experimental data. Solid curve a and broken curve b are due to eq 22 and $g_{12} = 1.51$, respectively. Broken curve c is due to eq 22 and 24.

deviate considerably from the expected vapor pressure 200 mmHg. Second, we calculated the total vapor pressures by using $g_{12} = 1.51(T_0/T)$ due to $h_{12} = 473$ and neglect of the entropy term. This result is given by broken curve b in Figure 2b. Broken curve a indicates a large entropic contribution to the function g_{12}. The behavior of broken curves a and b suggests that total vapor pressure is sensitive to the functional form of $g_{12}(u_2)$ but would be represented by a modified functional form of eq 18. Then we determined the function $g_{12}(T_0,u_2)$ in eq 21 in such a way that the total vapor pressure settled down to the constant value of 200 mmHg. Thus we obtained the function g_{12} in the form

$$g_{12} = (T_0/T - 1)[0.466 + 0.517/(0.119 + u_2)] + 2.08/(0.771 + u_2) \quad (22)$$

which gives the open circles in Figure 2b. The vertical bars for the calculated points indicate an uncertainty corresponding to the boiling temperature variation of ±0.5 °C. As described by the solid curve the total vapor pressure due to eq 22 is very close to the experimental value of 200 mmHg over the whole range of u_2. However, on account of the assumed temperature dependence in eq 21, eq 22 could be an approximate expression at large u_2. In the range of $u_2 < 0.75$, in which the boiling temperature does not exceed 55 °C, eq 22 could be accurate enough to analyze the second virial coefficients in the mixed solvent.

V. Comparison with the Generalized Flory–Huggins Equation

Since the interaction functions g_{ij} were determined with the experimental data, we can calculate A_2° by eq 6 with the aid of eq 8–12. First, we have ignored the contribution from the ternary function g_T in the calculation of A_2°. The results of the calculation are given by curve a in Figure 3. The calculated A_2° shows negative values in the region $u_2 < 0.2$ and except in this region has very large values. For comparison, we tried to calculate A_2° for the constant value of $g_{12} = 1.51$, which is comparable with the value due to the solubility parameter. Broken curve b in Figure 3 obtained by this calculation does not show negative values and has about the same values as solid curve a when $u_2 > 0.5$. The negative values of A_2° due to eq 22 are caused by the u_2 dependence of g_{12}. The very different behavior of solid curve a and the open circles of the experimental data manifests a large contribution from the ternary function g_T.

As eq 6 and 7 are derived at the limit of zero polymer concentration, an appropriate function of g_T is given by the equation

$$g_T(u_2,\phi_3) = g_T^\circ + (\partial g_T/\partial \phi_3)^\circ \phi_3 \quad (23)$$

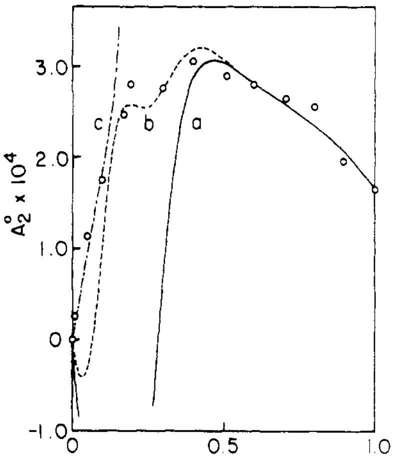

Figure 4. Plot of A_2° against the volume fraction u_2 of 2-methoxyethanol on an enlarged scale. Open circles represent the experimental data. Solid curve a is due to eq 22 and 24. Broken curve b is due to eq 22 and 25. Chain curve c is due to eq 22 and 24, and $(\partial g_T/\partial \phi_3)^\circ = 0.97$.

where g_T° and $(\partial g_T/\partial \phi_3)^\circ$ are functions of u_2. If both the quantities A_2 and λ are measured as a function of u_2, both the function of g_T° and $(\partial g_T/\partial \phi_3)^\circ$ can be determined with eq 6 and 7. That is, since eq 7 contains only the function g_T° and its derivative $(\partial g_T^\circ/\partial u_2)$, the function $g_T^\circ(u_2)$ can be evaluated from the data of λ. Once the function $g_T^\circ(u_2)$ is determined, the function $(\partial g_T/\partial \phi_3)^\circ$ can be evaluated from the data of A_2 with eq 6. However, in the present study the values of λ can not be determined on account of the isorefractive solvent pair and therefore only a qualitative argument about g_T can be made. In a following analysis we tried to show that the term of the ternary function in eq 5 is a relevant one to solve the large discrepancy between the experimental points and the calculated curve a in Figure 3.

First, by neglecting the derivatives $(\partial g_T/\partial u_2)^\circ$ and $(\partial g_T/\partial \phi_3)^\circ$ we evaluated the values of g_T at each u_2, which forces an agreement between eq 6 and the experimental values of A_2°. In this calculation eq 6 could not fit to the experimental values in the region of $u_2 < 0.3$, which indicated a large contribution from the derivative $(\partial g_T/\partial u_2)^\circ$. Then the relation between the evaluated g_T° and u_2 in the range $u_2 < 0.3$ was represented by a simple equation to estimate the derivative $(\partial g_T/\partial u_2)^\circ$, values of which were used for the next calculation of g_T similar to the foregoing one. By this method the experimental values of A_2° in the range $u_2 < 0.4$ was found to be represented by the equation

$$g_T = 1.04 - 0.58u_2 \quad (24)$$

Broken curve c in Figure 3 is described with eq 22 and 24. A_2° is described on enlarged scale in Figure 4, in which solid curve a is due to eq 22 and 24. The disagreement at $u_2 < 0.3$ is not improved by the introduction of eq 24. In order to force an agreement in $u_2 < 0.3$, a large positive value of $(\partial g_T/\partial u_2)^\circ$ was required and therefore the function g_T° must increase rapidly with increasing u_2 at small u_2. This situation can be seen by the relation

$$g_T^\circ = \{0.35/[0.35 + \exp(-15u_2)]\}(1.04 - 0.58u_2) \quad (25)$$

in which the front factor on the right-hand side is 0.259 at $u_2 = 0$ and becomes substantially unity at $u_2 = 0.4$. The calculated values of A_2° with eq 22 and 25 are given by broken curve b in Figure 4. The agreement between the observed and calculated values of A_2° is considerably improved, though the calculation still yields negative values at very small u_2 and an unexpected shoulder emerges near

$u_2 = 0.2$. The behavior of the calculated $A_2°$ was very sensitive to the choice of the numerical factors in eq 25. The above situation indicates that the observed $A_2°$ cannot be satisfactorily represented by the function $g_T°(u_2)$ alone and a reasonable agreement between the experimental and calculated values of $A_2°$ would be done with both the functions of $g_T°$ and $(\partial g_T/\partial \phi_3)°$. For the function $g_T°$ given by eq 24 we could easily determine the function $(\partial g_T/\partial \phi_3)°$ to force an agreement between the observed and calculated values of $A_2°$. The obtained $(\partial g_T/\partial \phi_3)°$ was about unity in $u_2 < 0.1$ and decreased rapidly with increasing u_2, vanishing near $u_2 = 0.4$. Chain curve c in Figure 4 was obtained with eq 22 and 24 and $(\partial g_T/\partial \phi_3)° = 0.97$. It became clear that the behavior of $A_2°$ of the present system can be reasonably explained by introducing the ternary function g_T given by eq 23, in which both the function $g_T°$ and $(\partial g_T/\partial \phi_3)°$ depend on u_2.

VI. Concluding Remarks

The observed second virial coefficient A_2 for the present ternary system was corrected for the excluded volume effect with the Kurata–Yamakawa theory[29] to compare it with the generalized Flory–Huggins equation. The comparison was made with the thermodynamic relation of eq 6, which has no approximations such as the single-liquid approximation. Since the binary functions g_{ij} were determined by the experiments on the binary systems of the components i and j, the large discrepancy between the experimental points and calculated curve a in Figure 3 is ascribed to the characteristic feature due to the mixed solvent. The ternary function given by eq 23 was found to be a relevant one to remove the discrepancy. The magnitude of the ternary function was predicted to be comparable with those of the functions g_{ij}, though a quantitative determination of the function was not feasible for lack of data of the preferential adsorption coefficient. According to the data analyses by the two-parameter theory, the effect of the ternary function was not reflected in the behavior of the universal function Ψ.[23] This could give a clue for a molecular explanation of the ternary function.

Large discrepancies between experimental data and calculations such as the difference between the data points and broken curve b in Figure 3 have been observed in intrinsic viscosities and second virial coefficients.[13,14,22] This discrepancy seems to be caused mainly by the neglect of the ternary function rather than the assumed constant values of g_{12}. The maximum value of $A_2°$ is not so sensitive to the values of g_{i3}. Therefore, as long as we use a relatively high value of g_{12} and neglect a ternary function, we could easily have a very large value of $A_2°$ as seen from eq 6–12. High values of g_{12} are expected for usual solvent mixtures from data of heats of mixing. However, we are not aware of such large experimental values of $A_2°$. Therefore, large effects of the ternary function on the thermodynamic properties of ternary systems appear to be rather common phenomena. It would be interesting to investigate the reason why the ternary function acts as to diminish the second virial coefficients to the same magnitude as those in single solvents.

References and Notes

(1) P. C. Deb and S. R. Palit, *Makromol. Chem.*, **166**, 227 (1973).
(2) B. A. Wolf and R. J. Molinari, *Makromol. Chem.*, **173**, 241 (1973).
(3) B. A. Wolf and G. Blaum, *J. Polym. Sci., Polym. Phys. Ed.*, **13**, 1115 (1975).
(4) G. Blaum and B. A. Wolf, *Macromolecules*, **9**, 579 (1976).
(5) I. Fernândez-Piērola and A. Horta, *Makromol. Chem.*, **182**, 1705 (1981).
(6) A. Horta and I. Fernândez-Piērola, *Polymer*, **22**, 783 (1981).
(7) R. H. Ewart, C. P. Roe, P. Debye, and J. R. McCartney, *J. Chem. Phys.*, **14**, 687 (1946).
(8) R. L. Scott, *J. Chem. Phys.*, **17**, 268 (1949).
(9) A. R. Shultz and P. J. Flory, *J. Polym. Sci.*, **15**, 231 (1955).
(10) B. E. Read, *Trans. Faraday Soc.*, **56**, 382 (1960).
(11) C. Strazielle and H. Benoit, *J. Chim. Phys. Phys.-Chim. Biol.*, **58**, 675, 678 (1961).
(12) J. Pouchlý, A. Živný, and K. Šolc, *J. Polym. Sci., Part C*, **23**, 245 (1968).
(13) A. Dondos and D. Patterson, *J. Polym. Sci., Part A-2*, **7**, 209 (1969).
(14) P. Munk, M. T. Abijaoude, and M. E. Halbrook, *J. Polym. Sci., Polym. Phys. Ed.*, **16**, 105 (1978).
(15) I. Prigogine, "The Molecular Theory of Solutions", North-Holland Publishing Co., Amsterdam, 1957, Chapter XVI.
(16) D. Patterson and G. Delmas, *Trans. Faraday Soc.*, **65**, 708 (1969).
(17) P. J. Flory, R. A. Orwoll, and A. Vrij, *J. Am. Chem. Soc.*, **86**, 3507, 3515 (1964).
(18) A. Horta and I. Fernândez-Piērola, *Macromolecules*, **14**, 1519 (1981).
(19) J. Pouchlý and D. Patterson, *Macromolecules*, **9**, 574 (1976).
(20) S. G. Chu and P. Munk, *Macromolecules*, **11**, 879 (1978).
(21) T. M. Aminabhavi and P. Munk, *Macromolecules*, **12**, 607 (1979).
(22) R. M. Masegosa, M. G. Prolongo, I. Hernândez-Fuentes, and A. Horta, *Macromolecules*, **17**, 1181 (1984).
(23) M. Nakata and N. Numasawa, *Macromolecules*, preceding paper in this issue.
(24) R. C. Reid, J. M. Prausnitz, and T. K. Sherwood, "The Properties of gases and Liquids", 3rd ed., McGraw-Hill, New York, 1977.
(25) W. H. Stockmayer, *J. Chem. Phys.*, **18**, 58 (1950).
(26) J. G. Kirkwood and R. J. Goldberg, *J. Chem. Phys.*, **18**, 54 (1950).
(27) H. C. Brinkman and J. J. Hermans, *J. Chem. Phys.*, **17**, 574 (1949).
(28) P. J. Flory, "Principles of Polymer Chemistry", Cornell University Press, Ithaca, NY, 1953.
(29) H. Yamakawa, "Modern Theory of Polymer Solutions", Harper and Row, New York, 1971.